Photodissociation dynamics of ethyl ethynyl ether: A new ketenyl radical precursor

M. J. Krisch, J. L. Miller, and L. J. Butler[a)]
James Franck Institute and Department of Chemistry, The University of Chicago, Chicago, Illinois 60637

H. Su and R. Bersohn
Department of Chemistry, Columbia University, New York, New York 10027

J. Shu
Chemical Sciences Division, Lawrence Berkeley National Laboratory, Berkeley, California 94720

(Received 22 January 2003; accepted 3 April 2003)

The work presented here investigates the dynamics of the photodissociation of ethyl ethynyl ether at 193.3 nm with photofragment translational spectroscopy and laser-induced fluorescence. The data from two crossed laser-molecular beam apparatuses, one with vacuum ultraviolet photoionization detection and one with electron bombardment detection, showed that only cleavage of the C–O bond to form a C_2HO radical and a C_2H_5 (ethyl) radical occurs. We observed neither cleavage of the other C–O bond nor molecular elimination to form $C_2H_4+CH_2CO$ (ketene). The C_2HO radical is formed in two distinct product channels, with 37% of the radicals formed from a channel with recoil kinetic energies extending from about 10 to 70 kcal/mole and the other 63% formed from a channel with lower average recoil energies ranging from 0 to 40 kcal/mole. The measurements using photoionization detection reveal that the C_2HO radical formed in the higher recoil kinetic-energy channel has a larger ionization cross section for photon energies between 10.3 and 11.3 eV than the radical formed in the lower recoil kinetic-energy channel, and that the transition to the ion is more vertical. The radicals formed in the higher recoil kinetic-energy channel could be either $\tilde{X}(^2A'')$ or $\tilde{A}(^2A')$ state ketenyl (HCCO) product and the shape of the recoil kinetic-energy distribution fitting this data does not vary with ionization energy between 10.3 and 11.3 eV. The C_2HO formed in the channel with the lower kinetic-energy release is likely the spin forbidden $\tilde{a}(^4A'')$ state of the ketenyl radical, reached through intersystem crossing. The $\tilde{B}$ state of ketenyl is energetically inaccessible. We also consider the possibility that the lower kinetic-energy channel forms two other C_2HO isomers, the CCOH (hydroxyethynyl) radical or the cyclic oxiryl radical. Signal from laser-induced fluorescence of the HCCO photofragment was detected at the electronic origin and the 5_1^0 band. The fluorescence signal peaks after a 20 μs delay, indicating that HCCO is formed with a significant amount of internal energy and then subsequently relaxes to the lowest vibrational level of the ground electronic state. The data show that the photodissociation of ethyl ethynyl ether produces C_2HO with unit quantum yield, establishing it as the first clean photolytic precursor of the ketenyl radical, a key species in combustion reactions. © *2003 American Institute of Physics*. [DOI: 10.1063/1.1577318]

I. INTRODUCTION

This paper investigates the photodissociation dynamics of ethyl ethynyl ether ($HCC–O–CH_2CH_3$) at 193.3 nm, establishing it as a unit quantum yield photolytic precursor of the C_2HO radical. The data show that C_2HO product is formed via two distinct channels, one which produces $\tilde{X}/\tilde{A}$ state HCCO and another giving the radical in an electronically or isomerically distinct state. Analysis of these product channels raises interesting questions of electronic accessibility.

The HCCO isomer, known as the ketenyl radical, acts as an intermediate in a wide range of combustion reactions. It is formed as an intermediate in the dominant oxidation pathway of acetylene, according to the reaction

$$C_2H_2+O(^3P)\rightarrow HCCO+H. \quad (1)$$

This pathway was first proposed by Fenimore and Jones in 1963[1] and has since been observed and studied extensively.[2,3] The ketenyl radical can go on to form highly reactive singlet methylene ($^1CH_2$) in rich flames, according to the reaction

$$H+HCCO\leftrightarrow {}^1CH_2+CO. \quad (2)$$

Reactions of singlet methylene are thought to open up pathways to the formation of higher hydrocarbons.[4] Since acetylene is found as an intermediate in flames from a wide range of fuels, the combustion community has a strong interest in the chemistry of the HCCO radical. For example, a recent study by Rim and Hershberger[5] investigated the product branching in HCCO+NO, a key reaction in the NO-reburning mechanism for the reduction of NO_x emissions from fossil fuel combustion.

a)Electronic mail: l-butler@uchicago.edu

Since there are many systems in which it is desirable to study the role of HCCO, a method is needed to cleanly produce the radical. Different procedures have been used, but all present complications. Ketenyl production through the photolysis of ketene, which was discovered by Unfried *et al.*[6] is currently the most commonly used method, proceeding according to the reaction:

$$CH_2CO + h\nu(193.3\ \text{nm}) \rightarrow CH_2(^3B_1) + CO, \quad (3a)$$

$$\rightarrow CH_2(^1A_1) + CO, \quad (3b)$$

$$\rightarrow HCCO + H, \quad (3c)$$

$$\rightarrow C_2O + H_2. \quad (3d)$$

The reaction, however, has only a 0.107 quantum yield of ketenyl radical [Eq. 3(c)] according to a recent study by Glass *et al.*[7] The photochemical reaction also produces triplet and singlet methylene [Eqs. 3(a) and 3(b)] with quantum yields of 0.628 and 0.193, respectively, as well as C_2O with a 0.072 quantum yield.[7] The fact that methylene is a product of the photolysis of this precursor [Eqs. 3(a) and 3(b)] has prohibited the accurate detection of the elementary reaction rates of the ketenyl radical. The methylene generated by ketene photolysis can not only complicate detection of the ketenyl-produced methylene [Eq. (2)], but can often react with other species to produce common reaction products with ketenyl radical reactions. Other groups have reacted oxygen atoms with acetylene to produce HCCO [Eq. (1)], but this reaction is slow at moderate temperatures and also produces methylene.[3] Abstraction of a hydrogen from ketene has been investigated as another possible source of the HCCO radical by Grußdorf *et al.*[8] for ketene reacted with F, Cl, and OH, as well as by Edwards and Hershberger[9] for ketene reacted with CN and NCO. In all cases, however, hydrogen abstraction appeared to be a minor or negligible reaction channel.

In analogy to methyl vinyl ether photodissociation, in which fission of the $O-CH_3$ bond was the only product channel observed,[10] HCCO production through photolysis of the $O-C_2H_5$ bond could potentially be the dominant product channel in ethyl ethynyl ether photodissociation. The use of organic ethers as precursors for radicals containing H, C, and O, including a proposal for generating HCCO, has been discussed by Bersohn.[11] The study presented here investigates the photodissociation dynamics of ethyl ethynyl ether and evaluates the molecule for use as an HCCO precursor. Of the energetically allowed product channels, the potential contributors to product branching, chosen in analogy to other hydrocarbon ether reactions, are

$$HCC-O-CH_2CH_3 + h\nu(193.3\ \text{nm})$$

$$\rightarrow HCCO + CH_2CH_3, \quad (4a)$$

$$\rightarrow HCC + OCH_2CH_3, \quad (4b)$$

$$\rightarrow CH_2CO + CH_2CH_2. \quad (4c)$$

A nonphotochemical analog to reaction (4c) has been studied in ethyl vinyl ether ($CH_2CH-O-CH_2CH_3$),[12] which forms ethylene and acetaldehyde upon thermal decomposition. Molera *et al.* (1968)[12] investigated the question of whether the molecular elimination channel in ethyl vinyl ether proceeded via a four- or six-center transition state. In the case of the four-center transition state, the ethylene would be formed upon H atom transfer from the CH_2 group of CH_2CH_5 to the vinyl group. The ethylene from the six-center transition state would be formed from the original CH_2CH_3 group upon H atom transfer to the vinyl group from the CH_3 group of the C_2H_5. When radioactive isotope tracers were attached to the precursor molecule, six-center elimination was revealed as the dominant dissociation pathway. Thus it is interesting to examine whether an analogous elimination via a six-center intermediate will occur in ethyl ethynyl ether, with an H atom being transferred from the CH_3 group of C_2H_5 to the ethynyl group. An analogous six-center transition state is not possible in methyl vinyl ether, and indeed a photofragmentation study on that molecule showed no molecular elimination channel.[10]

Apart from its role in combustion, the ketenyl radical is theoretically interesting as an example of a Case C Renner–Teller molecule in the classification system of Lee *et al.*[13] The Renner–Teller effect arises from an interaction between the vibrational and electronic angular momenta which produces a splitting of degenerate electronic energy levels as the molecule bends. The lowest energy Renner–Teller pair of states in the ketenyl radical consists of a ground state, $\tilde{X}(^2A'')$, with a bent equilibrium geometry, and a low-lying excited state, $\tilde{A}^2\Pi(^2A')$, with a linear equilibrium geometry. The exact structure of the ground-state radical has been a subject of discussion. Theoretical estimates of the radical's equilibrium geometry are sensitive to the manner in which electron correlation is incorporated into computational models, as first demonstrated by Goddard[14] and later confirmed in other studies.[15,16] The CC bond length and CCH bond angle are particularly sensitive to electron correlation and were later shown to also be highly dependent on the choice of basis set used.[16] In a study by Szalay *et al.*[16] the best estimate of the $\tilde{X}(^2A'')$ state geometry gave an HCC bond angle of $\sim 134.6°$ and an angle of $\sim 169.4°$ along the CCO bond. The microwave spectra obtained by Endo and Hirota,[17] show that the equilibrium geometry of the first excited state, $\tilde{A}^2\Pi(^2A')$, is linear. Szalay and Blaudeau[18] combined their theoretical estimate of the spin-orbit splitting in HCCO with data from the microwave spectra of the radical and calculated that the $\tilde{A}$ state lies only 3.359 kcal/mole above the minimum of the ground state. Both the $\tilde{X}$ and the $\tilde{A}$ states have most of the radical electron density centered around the carbon next to the hydrogen. Because fission of the $HCCO-C_2H_5$ bond in ethyl ethynyl ether would diabatically favor producing HCCO with the unpaired electron density on the O atom, clearly a substantial change in electron density must occur for ground electronic state HCCO to be the dominant product. The electronically facile product[19] would be $\tilde{B}$ state HCCO; the $v=0$ level of the $\tilde{B}$ state is located 95.6799 ± 0.0002 kcal/mole above the $v=0$ level of the ground state and has the radical electron density centered around the oxygen.[20,21] It would be interesting to see if nonadiabatic electronic behavior leads to a larger branching to $\tilde{B}$ state radical than energetic considerations alone would predict, but

unfortunately these experiments do not put enough energy into the system to evaluate this question. The other state of interest is the lowest quartet state, $\tilde{a}(^4A'')$, which has been predicted to lie 54.2 kcal/mole about the ground state.[22] The occurrence of an intersystem crossing in ethyl ethynyl ether would be necessary in order to produce $\tilde{a}$ state product.

This paper reports an investigation of the photodissociation dynamics of ethyl ethynyl ether. We present laser induced fluorescence (LIF) spectra taken at Columbia University and photofragment translational spectra taken at the University of Chicago and Lawrence Berkeley National Laboratory. The data reveal that ethyl ethynyl ether photodissociates cleanly to give C_2HO in two different electronic states or isomeric forms.

II. EXPERIMENT

The LIF experiments at Columbia were carried out in a standard apparatus, a stainless steel gas cell containing ethyl ethynyl ether which was irradiated first through one window with a 193.3 nm laser and, after a delay, through a second window by a probing frequency-doubled Nd:YAG-pumped dye laser. Signal was collected with a photomultiplier (PMT), through a Stanford Research Systems Gated Integrator and Boxcar Averager. In overlapping scans with two different dyes, the region from 298 to 320 nm was surveyed. The total pressure of the gas, which was a mixture of the ether and solvent hexane, was 100 mTorr.

The distribution of recoil velocities of ethyl ethynyl ether photofragments resulting from 193.3 nm photodissociation were measured in two different crossed laser-molecular scattering apparatuses. In one laboratory, located at the University of Chicago, photofragments were detected with electron bombardment ionization. In the other, Endstation 1 of the Chemical Dynamics Beamline of the Advanced Light Source (ALS) at the Lawrence Berkeley National Laboratory, a tunable VUV photoionization detector was employed. In both apparatuses, photodissociation occurs at an ''interaction region'' in which a laser beam intersects a molecular beam source. The laser beam comes in perpendicular to the plane containing the molecular beam and the line from the interaction region to the detector. The source region containing the molecular beam nozzle rotates, so data can be collected at a variety of source angles, defined as the angle between the molecular beam direction and the line from the interaction region to the detector. Photodissociation products scatter into many angles; the apparatus samples only the small portion of products with lab velocities pointed along the interaction region to detector line within the 1.5° acceptance angle of the detector. In the Chicago system, these photolysis products travel 44.6 cm to a ''universal detector'' in which the 200 eV electrons used for ionization contain enough energy to ionize and potentially fragment any neutral photofragment. The ions pass through a quadrupole mass spectrometer with a Model 13 High-Q head from Extrel [resolution set to 1.0 amu full width at half maximum (FWHM)]. The mass-selected ions are detected by a Daly detector, and the resultant voltage pulses are counted by a multi-channel scaler. This gives the number of ions at each mass to charge ratio produced from the neutral photofragments arriving at the detector as a function of time after the dissociating light pulse. An ion flight constant of $\alpha=4.5$ $\mu s/amu^{1/2}$ is used to correct for the portion of the photofragment's travel during which it is an ion, giving a neutral time of flight for the data analysis. The time-of-flight spectra of the neutral photofragments are forward convolution fit to determine the distribution of energies partitioned to photofragment recoil translational energy.

The second apparatus used was Endstation 1 on the Chemical Dynamics Beamline at the Advanced Light Source (ALS) in Lawrence Berkeley National Lab. The set-up is similar to the one described above, but with tunable, VUV photoionization. A detailed description of this apparatus is given elsewhere.[23] Relevant parameters for this experiment are the total interaction region to detector distance, which is 15.1 cm, the time-of-flight constant of 7.02 $\mu s/amu^{1/2}$, and the detector acceptance angle of 1.3°. A 2.1 MHz quadrupole was used, with resolution that varied slightly with mass and was set to avoid problems of mass leakage at all masses of interest. The FWHM was 0.36 amu at $m/e=41$ and narrower at lower masses; for example, the FWHM at $m/e=29$ was 0.3 amu. The synchrotron radiation was generated with a U10 undulator and tuned through changes in the undulator gap. In addition to radiation at the wavelength of interest, higher harmonic light is generated. An argon gas filter helped to block out these higher harmonics and for photoionization energies below 10.6 eV (corresponding to an undulator gap of 27.8175 mm) a MgF_2 window was also used as a filter. In many cases, however, these filters were not sufficient, so the laser was run at half the repetition rate of the pulsed valve and the data collected with valve on, laser off were subtracted out as background. The photoionization energies quoted here are determined from the undulator gap and related to the energy by a recent calibration done with a 3 m McPherson monochrometer with a 600 groove/mm grating.[24] This is not equivalent to the values given by the beamline ''calculator,'' which were typically reported in previous publications from this apparatus and which deviate significantly from the true value in some cases. For example, when the beamline calculator is set to give 12.5 eV, the actual peak energy is about 0.2 eV lower than that. For all of the spectra taken here, beam defining apertures of 10 mm×10 mm were used to spatially select a portion of the ALS beam, giving a total spectral bandwidth of about 5% FWHM. Most of the width beyond 2.3% FWHM, however, arose from a long tail extending out to the red.[24]

The ethyl ethynyl ether was obtained as a 50% solution in hexanes from Acros Chemicals and used without further purification. The hexanes have negligible absorption at 193.3 nm. At Chicago the sample was kept at a temperature of −15.0 °C. The vapor at equilibrium with the solution was seeded in He to a total backing pressure of 330 Torr and expanded through a 200 °C continuous nozzle into the vacuum chamber. The nominal nozzle diameter was 0.10 mm, but it was found at the conclusion of the experiment to have expanded through corrosion. At the ALS, the solution was kept at −15.5 °C and the vapor at equilibrium with the solution, seeded in helium for a total pressure behind the nozzle of 400 Torr, was expanded through a pulsed nozzle of

1 mm diameter and 180 μs pulse length, heated to 114 °C. The nozzle temperature used at the ALS was not high enough to completely eliminate clusters, as will be discussed later.

The 193.3 nm light was produced from the ArF transition of an unpolarized excimer laser. The Chicago data were collected at an energy of 15 mJ pulse^{-1} focused onto a 8.4 mm^2 spot, whereas the ALS data were taken at ~25 mJ pulse^{-1} focused onto a 16.3 mm^2 spot. Power studies from 15 to 60 mJ at the ALS indicated that 25 mJ lay within a region of single photon transitions, in which signal intensity varied linearly with laser power. Data collected, but not presented here, at higher powers (up to 150 mJ/pulse) at Chicago were suggestive of multi-photon processes in this power range, but low signal to noise prevented a full power study.

Signal from the photofragmentation of ethyl ethynyl ether was detected at $m/e=41\,(C_2HO^+)$, $25\,(C_2H^+)$, and $27\,(C_2H_3^+)$, $29\,(C_2H_5^+$; this m/e ratio could also correspond to CHO^+, see Results and Analysis section for assignment). No evidence of signal at $m/e=42\,(C_2H_2O^+)$ and $45\,(C_2H_5O^+)$ was found (see Results and Analysis section). Although ALS signal from the photodissociation of clusters was not detected for parent mass at 10° and 7.5° when averaged for 15 000 laser shots, evidence for clusters was detected in a small, slow shoulder in the ALS data at $m/e=29$ which became larger at a lower nozzle temperature.

Calculations to find the bond dissociation energy of ethyl ethynyl ether were performed using GAUSSIAN 98[25] at the G3//B3LYP level of theory, as described by Baboul *et al.*[26] The September 2001 version of GAMESS[27] was used to calculate transition moments and spin–orbit coupling matrix elements between different electronic states of ethyl ethynyl ether. These calculations used singlet and triplet reference wavefunctions generated at the unrestricted Hartree–Fock (UHF)/6-311G** level of theory and configuration interaction (CI) singles excitations from those wavefunctions, at the geometry of the planar conformer.

III. RESULTS AND ANALYSIS

A. Laser induced fluorescence

Laser induced fluorescence experiments sought to detect the HCCO product of ethyl ethynyl ether photodissociation. In analogy with the extensive hot bands found with vinoxy, a rich set of hot bands was expected in the $\tilde{X}\rightarrow\tilde{B}$ LIF HCCO excitation spectrum and a wide scan was carried out in order to detect the singly excited vibrational states of all modes except for the C–H stretch. However, as shown in Fig. 1, in addition to the electronic origin, the (0,0) band at 33 424 cm^{-1}, the only hot band observed (with distinctly poorer signal strength) was the 5_1^0 band 491 cm^{-1} to the red. These were also the only bands observed in the previously reported LIF work of Brock *et al.*[20,21] They reported a very low fluorescence yield. The new finding is that the fluorescent signal intensity is very weak soon after the photodissociation but increases to a maximum at a delay time of about 20 μs and after that slowly decays, presumably due to diffusion of the radical away from the probed region. The time dependence

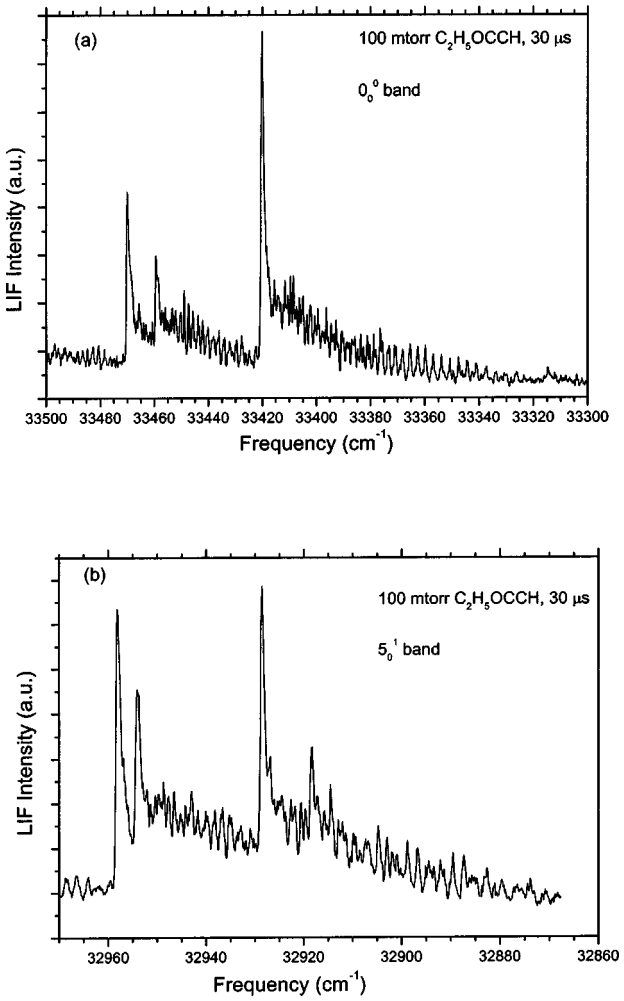

FIG. 1. (a) LIF excitation spectrum of the (0,0) band. (b) LIF excitation spectrum of the 5_1^0 band.

of the intensity of the peaks in the two spectra of Fig. 1 is shown in Fig. 2. The fact that little or no signal is seen at early times but is seen at later times means that the HCCO is formed in an intermediate dark state which is only slowly converted to the state which does exhibit LIF. The intermediate state may contain a large amount of vibrational or electronic energy, or both. There are two reasons for the sparse LIF spectrum. First, the fluorescence quantum yield is very small; and second, the LIF spectrum can only be seen at such long times that the HCCO has been vibrationally relaxed (by collisions with molecules of the precursor and the hexane solvent). Analysis of these LIF data cannot provide quantitative information about the amount of energy in the intermediate state(s), but the results are in qualitative agreement with the fragment kinetic-energy measurements in Sec. III B which indicate that there is a large amount of internal energy in the nascent HCCO radicals.

B. Photofragment translational spectroscopy

Photofragment translational energy spectra showed evidence for only one bond fission channel arising from ethyl ethynyl ether photolysis. All of the data could be fit by assuming that only cleavage of the HCCO–C_2H_5 bond to form

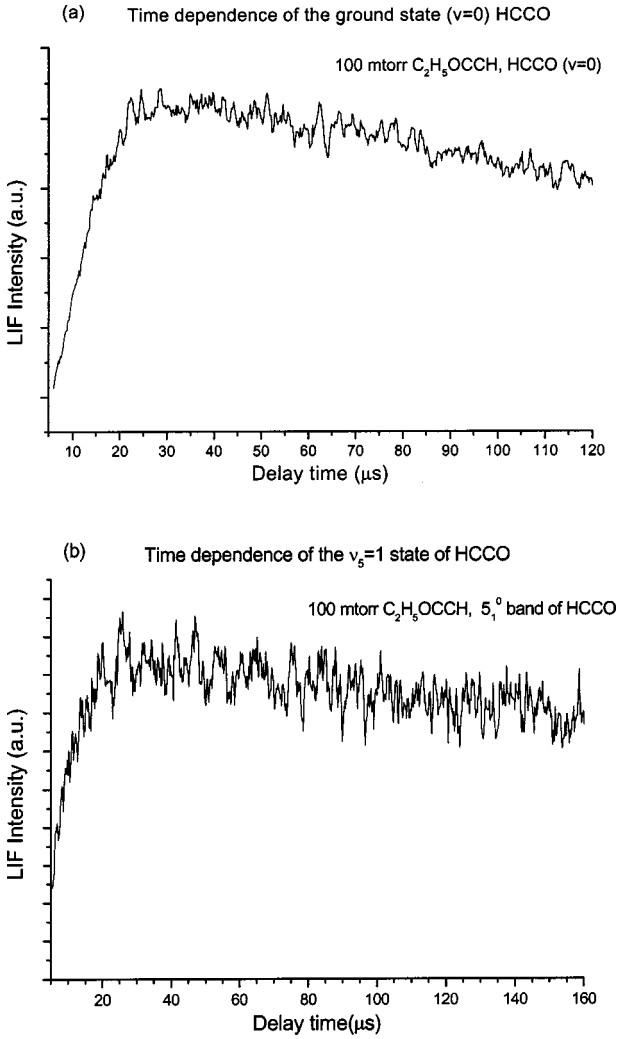

FIG. 2. (a) LIF excitation intensity of the (0,0) band as a function of time delay between the 193.3 nm laser pulse and the probe laser dye pulse. (b) LIF excitation intensity of the 5_1^0 band as a function of time delay between the 193.3 nm laser pulse and the probe dye laser pulse. Note that this signal is much weaker than that in the previous figure.

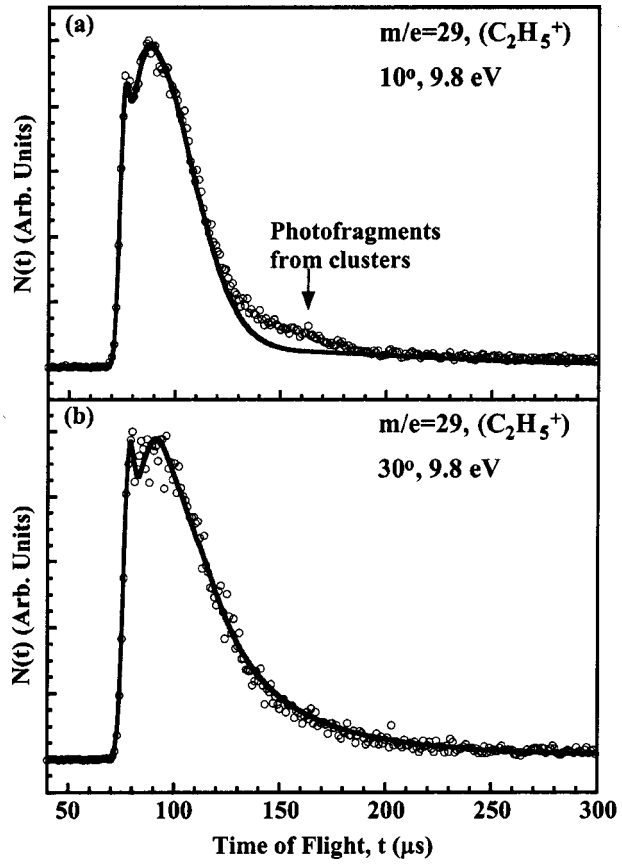

FIG. 3. TOF spectra at $m/e=29$ ($C_2H_5^+$) taken with a 9.8 eV photoionization energy (undulator gap at 26.6989 mm) with signal averaging for (a) 404 000 laser shots and (b) 150 000 laser shots. The source angle is set to (a) 10° and (b) 30°. The forward convolution fit to these data, shown with the solid line, was obtained from the $P(E_T)$ shown in Fig. 4. Experimental data points are given by the open circles. The bump in spectrum (a) marked as "photofragments from clusters" corresponds to low center-of-mass recoil velocities and became larger at lower nozzle temperatures.

C_2HO radical+ethyl (C_2H_5) radical occurred. Neither cleavage of the other C–O bond leading to $HCC+OC_2H_5$, nor elimination to give $C_2H_2+OCHCH_3$ was indicated. However, two electronically distinct C_2HO products were detected.

In order to detect the C_2H_5 ethyl radical with good signal to noise, time-of-flight (TOF) spectra were taken at $m/e=29$ at the ALS for two different source angles: 10° and 30° (Fig. 3). The $P(E_T)$ derived from forward convolution fitting of these TOF spectra is shown in Fig. 4; it is broad and bimodal. As will be discussed later, we found evidence that this $P(E_T)$ is actually the sum of two distinct $C_2HO+C_2H_5$ product channels. The $m/e=41$ (C_2HO^+) data (Fig. 5) from the universal detection system at Chicago is momentum matched to the $m/e=29$ data taken at the ALS with an ionization photon energy of 9.8 eV, indicating that these spectra correspond to the photolysis of $HCC–O–C_2H_5$ into $C_2HO+C_2H_5$. (i.e., in the center-of-mass reference frame, the recoil velocities of all the detected C_2HO fragments have a corresponding, $m_1\boldsymbol{v}_1=-m_2\boldsymbol{v}_2$, C_2H_5 fragment detected in the $m/e=29$ signal.) The momentum-matched fits also show that with high-energy electron bombardment the C_2HO produced is detected with a probability independent of its electronic or isomeric state, as are the C_2H_5 products.

The small, unfit bump that appears at long ion flight times in the $m/e=29$ data was determined to be from the photodissociation of clusters that persisted at the highest nozzle temperature possible under the running conditions at the ALS ($T_{\text{nozzle}}=114\,°C$). The position of the bump corresponds to low center-of-mass recoil velocities and this feature grows larger for an unheated nozzle. The data from the apparatus at Chicago were taken at nozzle temperatures of 200 °C, as calibrated with a helium TOF. No cluster products were observed at this higher temperature, although a small amount could be present but undetectable due to the lower signal to noise ratio.

We also looked for C–O fission leading to OC_2H_5 (mass 45) and HCC radical (mass 25). Signal was detected at Chicago at $m/e=25$ and 10° (Fig. 6), but was well fit by assuming it was due to cracking from mass 29 and mass 41. The fits shown in Fig. 6 assume that the C_2HO products from both $C_2HO+C_2H_5$ product channels have the same daughter ion cracking probability to $m/e=25$; this fits the data well.

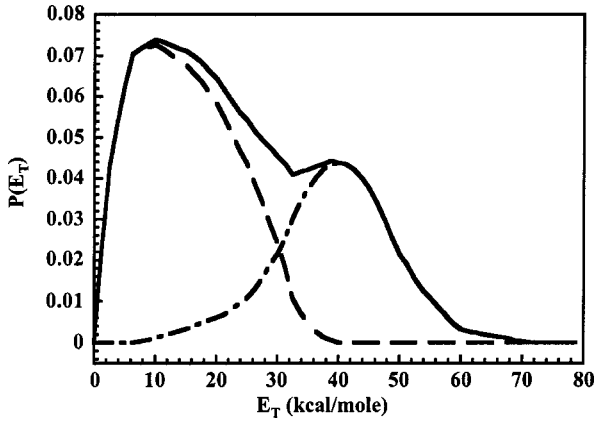

FIG. 4. The $P(E_T)$ for all HCCO–C_2H_5 bond fission events, derived from the forward convolution fit of the $m/e=29$ spectra in Fig. 3, is given by the solid line. Based on analysis of the $m/e=41$ (C_2HO^+) ALS spectra, this bimodal distribution was resolved into two components, one with low recoil kinetic energy (dashed line) and one high recoil kinetic energy (dot–dashed line), as discussed in the text.

Signal at $m/e=25$ was also detected at the ALS, but it exhibited an ionization energy dependence that will be discussed later. No evidence was found for any products at $m/e=45$. At Chicago, $m/e=45$ data were collected for 1.15 million laser shots, giving an integrated signal of -500 ± 1500. At the ALS, $m/e=45$ data at 10° were collected at 10.8 eV for 46 600 laser shots. The ionization energy for $O–CH_2CH_3$ is given as 9.11 eV.[28] The total, background subtracted signal was 8 ± 17 counts. Since nothing was seen at $m/e=45$ and 44, and the $m/e=25$ signal could be explained as daughter ion cracking from the ketenyl radical channel, we conclude that the OC_2H_5+HCC product channel does not contribute significantly to the product branching.

We also looked for an elimination channel which would produce ethylene (C_2H_4, mass 28)+ketene ($COCH_2$, mass 42). No peak was observed at $m/e=42$; the integrated signal was $-1.7*10^5 \pm 2.3*10^5$ after data collection for 2.5 million laser shots at Chicago. These data were taken at 150 mJ laser power, but lower power data taken for 1 million shots also showed no signal. The integrated signal was -880 ± 600 after data collection for 50 000 laser shots at the ALS. The ALS data were taken at a photoionization energy of 10.8 eV, whereas the ionization energy of ketene is 9.617 ± 0.003 eV.[29] No attempt was made to look for signal at $m/e=28$, as there is a very high background at this mass. Instead, data were collected in Chicago at a source angle of 10° at $m/e=27$ ($C_2H_3^+$), a dominant daughter of neutral C_2H_4 upon high-energy electron bombardment ionization.[30] A peak was found, but this was well fit by assuming that it was due entirely to daughter ions of the mass 29 (C_2H_5) photofragment (Fig. 7). Thus we conclude that bond fission to produce $HCOCH_2+C_2H_4$ does not contribute significantly to the product branching.

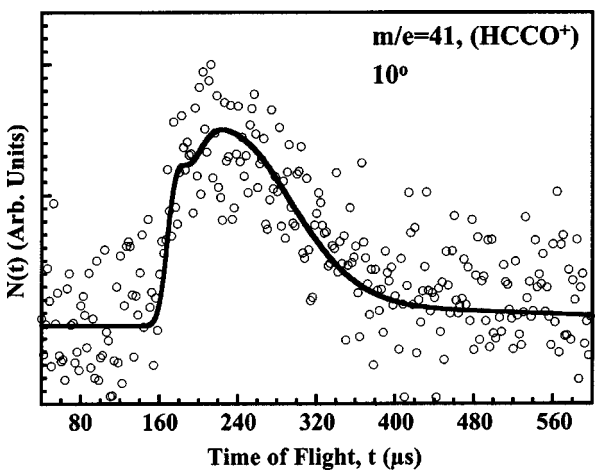

FIG. 5. TOF spectrum at $m/e=41$ (C_2HO^+) taken with 200 eV electron bombardment ionization at a source angle of 10°. Signal was averaged for 1.85 million laser shots. Open circles indicate experimental data and the solid line shows the forward convolution fit calculated from the $P(E_T)$ in Fig. 4.

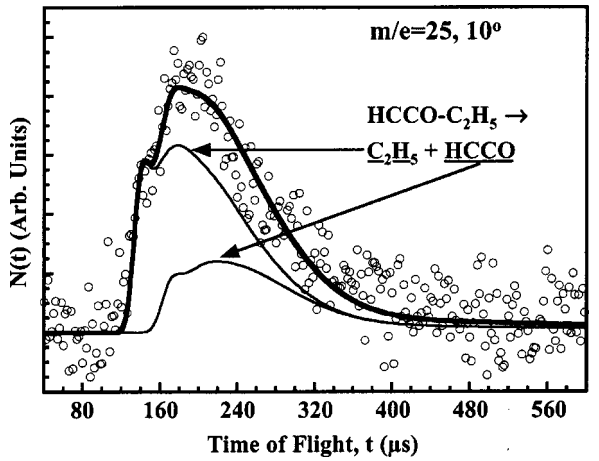

FIG. 6. TOF spectrum at $m/e=25$ (C_2H^+) taken with 200 eV electron bombardment ionization at a source angle of 10° with signal averaging for 2.5 million laser shots. Experimental data is shown with open circles. The thick solid line indicates the forward convolution fit obtained from the $P(E_T)$ in Fig. 4, assuming that the signal is from the $m/e=25$ daughter ion fragment of the ethyl radical (C_2H_5, thin line) and the $m/e=25$ daughter fragment of the ketenyl radical (HCCO, thin line).

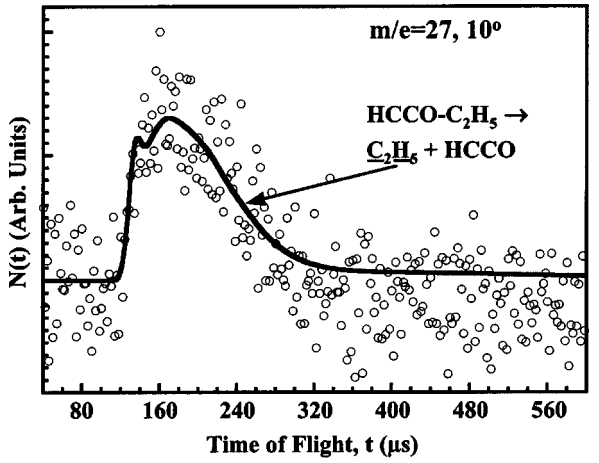

FIG. 7. TOF spectrum at $m/e=27$ ($C_2H_3^+$) taken with 200 eV electron bombardment ionization at a source angle of 10°. Signal was averaged for 3.5 million laser shots. Open circles indicate experimental data and the solid line shows the forward convolution fit calculated from the $P(E_T)$ in Fig. 4, assuming that all of the signal is from the ethyl radical fragmentation to $m/e=27$ in the electron bombardment ionizer.

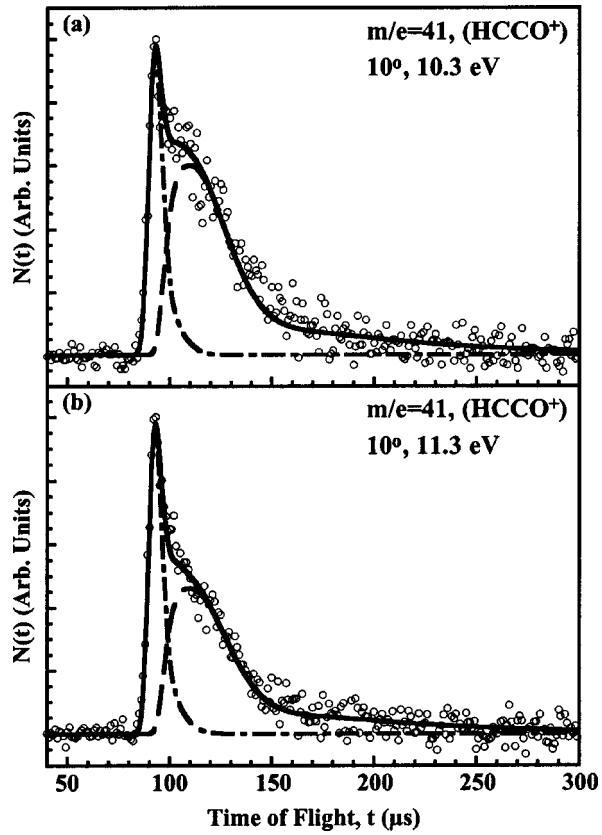

FIG. 8. TOF spectra at $m/e=41$ (C_2HO^+) taken at the ALS with photoionization energies of (a) 10.3 eV (undulator gap at 27.4102 mm) and (b) 11.3 eV (undulator gap at 28.7171 mm) and a source angle of 10°. Signal was averaged for 150 000 laser shots, with background subtraction, for both spectra. For the 10.3 eV spectrum (a) an additional MgF_2 window was used to filter out higher harmonics. Open circles indicate experimental data and the solid line indicates the forward convolution fit obtained from the $P(E_T)$ is shown in Fig. 4 with dot–dashed and dashed lines. The contribution from the high recoil kinetic-energy $P(E_T)$ is shown with the dot–dashed line and the contribution from the low recoil kinetic-energy $P(E_T)$ is shown with the dashed line. See the text for an explanation of the photoionization energy dependence of these components.

While the data clearly show that the only product channel is fission of the O–C_2H_5 bond, the bimodal $P(E_T)$ is evidence of two distinct mechanisms for forming $C_2HO + C_2H_5$. To further characterize the mass 41 (C_2HO) photofragment, we measured the $m/e=41$ TOF at two photon energies, 10.3 and 11.3 eV (Fig. 8). When we split the bimodal $P(E_T)$ into the two separate components shown in Fig. 4, changing the relative probabilities of the high recoil kinetic-energy component $P(E_T)$ and the low recoil kinetic energy component $P(E_T)$ allowed us to fit both of the ALS $m/e=41$ spectra. The fraction of HCCO–C_2H_5 bond fission events represented by the high recoil kinetic energy $P(E_T)$ in Fig. 4 is 37% while the fraction represented by the low recoil kinetic energy $P(E_T)$ is 63%. The data taken at different photoionization energies yield information about the relative photoionization cross sections of the C_2HO formed in each of these two product channels [Eq. (5)]. The branching ratio, $R=37\%/63\%$, of the high kinetic-energy channel to the low kinetic-energy channel is a constant for all the data, and is related to the apparent branching ratio ($\sigma^{\circ m/e=41}_{\mathrm{HKE}}/\sigma^{\circ m/e=41}_{\mathrm{LKE}}$) obtained by finding the relative signals at $m/e=41$ (C_2HO^+) at each photoionization energy.

$$R=\frac{\sigma_{\mathrm{HKE}}}{\sigma_{\mathrm{IKE}}}=\frac{\sigma^{\circ m/e=41}_{\mathrm{HKE}}}{\sigma^{\circ m/e=41}_{\mathrm{LKE}}}x\frac{Q_{\mathrm{LKE}}}{Q_{\mathrm{HKE}}}x\frac{f_{41}^{41\ \mathrm{LKE}}}{f_{41}^{41\ \mathrm{HKE}}}x\frac{T_{41}}{T_{41}}. \tag{5}$$

Here σ and σ° represent the actual and apparent cross sections and Q is the photoionization cross section of the C_2HO product, with HKE and LKE indicating the C_2HO product from high and low recoil kinetic-energy product channels, respectively. The term f_{41}^{41} is the daughter ion cracking fraction under the conditions used. Since the same two distributions fit the electron impact ionization data as well as the 10.3 and 11.3 eV data, the data show that the fraction of neutral mass 41 products which produce $m/e=41$ upon photoionization is roughly constant across the whole internal energy distribution of the C_2HO products for a given component $P(E_T)$. The ratio between the quadrupole transmission probabilities, T_{41}/T_{41}, is unity, as both the high kinetic-energy C_2HO and the low kinetic-energy C_2HO products are detected at $m/e=41$.

The ratio $\sigma_{\mathrm{HKE}}/\sigma_{\mathrm{LKE}}$ is found to be (1.0/1.7034) from the electron impact ionization data. To fit the 10.3 eV data we used $\sigma^{\circ m/e=41}_{\mathrm{HKE}}/\sigma^{\circ m/e=41}_{\mathrm{LKE}}=0.80$, and for the 11.3 eV data, $\sigma^{\circ m/e=41}_{\mathrm{HKE}}/\sigma^{\circ m/e=41}_{\mathrm{LKE}}=0.62$. Assuming that $f_{41}^{41\ \mathrm{LKE}}/f_{41}^{41\ \mathrm{HKE}}\approx 1$, this indicates that the C_2HO formed in the high recoil kinetic-energy channel has an ionization cross section that is 2.13 and 2.75 times larger than that of C_2HO in the low recoil kinetic-energy channel at 10.3 and 11.3 eV, respectively. This implies that, for the photon energies studied, the C_2HO formed in the high recoil kinetic-energy channel has a larger ionization cross section than the slow channel and one that increases more rapidly with photon energy; e.g., the fast C_2HO evidences a more vertical transition to the ion.

We conclude that there are two channels corresponding to HCCO–C_2H_5 fission, producing two forms of the C_2HO radical, each with a different variation in photoionization cross section with photon energy. This result is evidence of two distinct types of C_2HO photofragments, one that is produced with a faster recoil kinetic-energy distribution which extends from about 10 to 70 kcal/mole. We assign the higher recoil kinetic-energy distribution to C–O fission producing HCCO product in the Renner–Teller split $\tilde{X}$ and/or $\tilde{A}$ states (see Discussion). These ketenyl products are formed with a large range of internal energy, but the good fits of the data at 10.3 and 11.3 eV suggest that the ionization efficiency does not vary significantly with internal energy. The second product channel, which we infer to form a higher internal energy state or isomer of C_2HO, partitions less energy to product recoil. The slower kinetic-energy distribution extends from 0 kcal/mole to about 40 kcal/mole. The identity of this photofragment will be addressed in the discussion.

Information on the internal energy of the photofragments is obtained through conservation of energy:

$$E_{\mathrm{parent}}+E_{h\nu}=D_0(\mathrm{C–O})+E_{\mathrm{int}}+E_T. \tag{6}$$

Here E_{parent} is 1 to 2 kcal/mole due to cooling in the molecular beam and taken as zero for the rough calculation. $E_{h\nu}$ is the energy of the 193.3 nm excitation photon (148.0 kcal/mole with air-to-vacuum correction). We calculated the

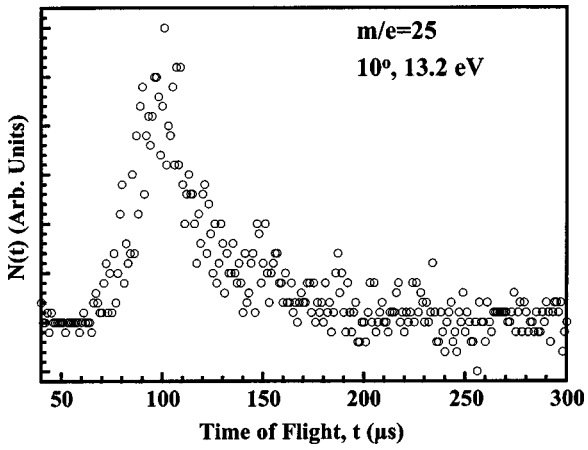

FIG. 9. TOF spectrum at $m/e=25$ taken with 13.2 eV photoionization energy (undulator gap at 30.9854 mm) and a source angle of 10°. Signal was background subtracted and, unlike the other data presented here, this spectrum was taken with an unheated nozzle. Open circles are experimental data points; see text for discussion.

bond energy, D_0, to be 51.4±2 kcal/mole using GAUSSIAN 98[25] at the G3//B3LYP level of theory.[26] In order to obtain this value, we calculated heats of formation at 0 K for ethyl radical, ketenyl radical, and ethyl ethynyl ether. The uncertainty for these calculations was 1 to 2 kcal/mole; see Baboul *et al.*[26] for an evaluation of the method against different test sets. We found $\Delta H_{f0}(C_2H_5)=31.3$ kcal/mole and $\Delta H_{f298}(C_2H_5)=28.8$ kcal/mole, as compared to an evaluated experimental value of $\Delta H_{f298}(C_2H_5)=28.4\pm0.5$ kcal/mole.[31] Our $\Delta H_{f0}(HCCO)=41.0$ kcal/mole and $\Delta H_{f298}(HCCO)=41.3$ kcal/mole were close to the literature value of $\Delta H_{f298}(HCCO)=42.2\pm0.7$ kcal/mole.[32,33] We found $\Delta H_{f0}(HCCO{-}C_2H_5)=20.9$ kcal/mole and $\Delta H_{f298}(HCCO{-}C_2H_5)=17.3$ kcal/mole, somewhat higher than the calculated literature value of $\Delta H_{f298}(HCCO{-}C_2H_5)=15.1$ kcal/mole.[34] The literature value was obtained through a semiempirical PM3 calculation that is expected to be less accurate than the G3//B3LYP method.[35] Using $D_0=51.4$ kcal/mole, we find $E_{avl}=96.6$ kcal/mole, where $E_{avl}=E_{int}+E_T$. Thus the products in the high recoil kinetic-energy channel have roughly 25–85 kcal/mole of energy partitioned to internal excitation. The low recoil kinetic-energy products partition between roughly 55 kcal/mole and the energetic limit of 96.6 kcal/mole of energy to internal excitation.

Data at $m/e=25$ (C_2H^+) were collected at the ALS at a photoionization energy of 13.2 eV, with an unheated nozzle (Fig. 9). We could not adequately fit these data by weighting the $P(E_T)$'s shown in Fig. 4 for the two $C_2HO+C_2H_5$ bond fission channels and assuming daughter ion cracking from ethylene (C_2H_5) and C_2HO radical, even though this approach fit the $m/e=25$ electron impact ionization spectrum. This indicates an internal energy dependence of the formation of $m/e=25$ upon photoionization, but this is a minor daughter ion upon low-energy photoionization.

IV. DISCUSSION

This study establishes that ethyl ethynyl ether is the first clean photolytic precursor of the ketenyl radical, producing C_2HO in approximately unit quantum yield. Unlike many previous methods of ketenyl radical production, methylene is not formed as a side product, which is particularly advantageous in studies where reactions of the ketenyl radical are expected to form methylene or when methylene reactions compete with ketenyl reaction mechanisms and produce a common product. In fact, the results from this study have already led to the use of ethyl ethynyl ether as a precursor of the ketenyl radical for a kinetics experiment by Osborn examining the $HCCO+O_2$ reaction.[36]

The 20 μs risetime in the laser induced fluorescence data clearly shows that the vibrationless $\tilde{X}$ state has very little initial population. This suggests that the initial energy distribution peaks at high internal energies. This is in keeping with the $P(E_T)$ measured by photofragment translational spectroscopy. The $P(E_T)$ shows no probability of forming $HC_2O+C_2H_5$ with more than 70 kcal/mole of energy in translation; in other words, only events which leave more than 25 kcal/mole of internal energy in the products have a significant probability of occurring. Keep in mind that 20 μs risetime in the laser induced fluorescence results reflects a combination of the relaxation of nascent HCCO that is vibrationally hot, and the relaxation of a second population that may be formed in either the quartet excited state or in a different C_2HO isomer.

The photofragment translational spectroscopy data reveal two $C_2HO+C_2H_5$ recoil kinetic-energy distributions. In order to identify the C_2HO product formed in each channel, we must examine which isomers and electronic states are energetically accessible given the range of internal energy present in each product derived from the measured recoil kinetic-energy distributions (Fig. 4). Recall that 96.6 kcal/mole of energy is available to the photofragments after C–O bond fission if they are formed in the ground electronic state. First we will examine the high recoil kinetic-energy products, which have roughly 25–85 kcal/mole of energy partitioned to internal excitation. Even at the highest kinetic energies obtained for this channel, the $C_2HO+C_2H_5$ products leave with at least 25 kcal/mole partitioned to internal energy of the fragments. Very little internal energy is imparted to vibrational energy of the ethyl fragment, whereas considerable vibrational energy may be partitioned to the HCCO fragment because electronic excitation primarily involves orbitals on the HCCO moiety. Note that conservation of angular momentum requires considerable energy to be partitioned to rotation when the recoil kinetic energy is near 70 kcal/mole. Thus, one would not expect to see the recoil kinetic energy $P(E_T)$ extend out to the energetic limit of 96.6 kcal/mole above the energy of zero-point $HCCO+C_2H_5$, as 20–30 kcal/mole should be partitioned to rotational energy of the two fragments. The $\tilde{X}$ and $\tilde{A}$ Renner–Teller split pair of states of the ketenyl radical are quite close in energy, differing by only 3.359 kcal/mole.[18] The high recoil kinetic-energy channel could produce either $\tilde{X}$ or $\tilde{A}$ state ketenyl radical; both states are energetically accessible, given the measured energy distribution. The $\tilde{a}$ and $\tilde{B}$ states of the ketenyl radical, as well as two higher energy isomers of C_2HO are discussed in the following paragraphs. With the excep-

tion of the oxiryl radical, whose energy is not well known, none of these products could explain the energy distribution of the high recoil kinetic-energy channel. All of them would require more than 25 kcal/mole of energy (as measured above the ground state of HCCO) for formation, and thus could not partition up to 70 kcal/mole to kinetic energy, as observed for this channel. The lowest energy possibility of this group, the $\tilde{a}$ state of the ketenyl radical, requires 54.2 kcal/mole more energy for formation than $\tilde{X}$ state product. Thus we conclude that the observed high recoil kinetic-energy channel forms the $\tilde{X}/\tilde{A}$ state ketenyl radical.

To identify the C_2HO product formed in the lower recoil kinetic energy channel, we consider that this channel partitions between roughly 55 and 96.6 kcal/mole of energy to internal excitation. It could not be forming $\tilde{A}$ state ketenyl radical as the 3.359 kcal/mole energy difference between the $\tilde{X}$ and $\tilde{A}$ states of ketenyl is too small to explain why no photofragments have less than about 55 kcal/mole of internal energy. At the Franck–Condon geometry of the HCCO moiety in ethyl ethynyl ether, the $\tilde{X}$ and $\tilde{A}$ states are almost exactly degenerate so one would not expect any significant extra partitioning of internal energy to the $\tilde{A}$ state products. (Indeed, a simple Franck–Condon calculation predicts 13 kcal/mole of vibrational energy in both the $\tilde{X}$ and $\tilde{A}$ states.) *Ab initio* calculations have predicted that the $\tilde{a}(^4A'')$ state of HCCO lies 54.2 kcal/mole above the ground state.[22] Forming this product from excitation to the singlet excited state of ethyl ethynyl ether would be spin forbidden, but the possibility of intersystem crossing remains. The $\tilde{a}(^4A'')$ state of HCCO is in the right range to account for the highest kinetic energies observed for the second $C_2HO+C_2H_5$ product channel, especially when the substantial uncertainty ($\sim$10 kcal/mole) regarding the high kinetic-energy edge of the low recoil kinetic-energy distribution is taken into account. The ketenyl radical $\tilde{B}$ state is just barely accessible with a 193.3 nm photon, at 95.6799 ± 0.0002 kcal/mole above the ground state,[20] but it is inaccessible for virtually all of the observed kinetic-energy distribution. Thus the most reasonable assignment of the products from the lower recoil kinetic energy channel is $HCCO\,\tilde{a}(^4A'')+C_2H_5$.

Both ground-state HCCO and $\tilde{a}(^4A'')$ HCCO can, in principle, dissociate to CH+CO at high internal energies, yet our experiments detect HCCO product from dissociation events that partition over 90 kcal/mole to internal energy. This stability of HCCO to secondary dissociation at high internal energies provides support for the conclusion that the HCCO formed in the low kinetic-energy distribution is in the $\tilde{a}(^4A'')$ state. While ground-state HCCO dissociates to $CH(X\,^2\Pi)+CO$, the only spin-allowed products from $\tilde{a}(^4A'')$ HCCO are $CH(a\,^4\Sigma^-)+CO$, with an energy of 17.1 kcal/mole above the $CH(X\,^2\Pi)+CO$ zero-point level.[37] The exit barrier to the quartet state dissociation is predicted to be small.[22,38] The $CH(a\,^4\Sigma^-)+CO$ products in the spin allowed dissociation channel have an asymptotic energy of 89.5 kcal/mole (72.4 kcal/mole[33] to $CH(X\,^2\Pi)+CO$ added to 17.1 kcal/mole). Thus HCCO formed from dissociation events partitioning 2 kcal/mole to translation (corresponding to $\sim$95 kcal/mole internal energy in $HCCO+C_2H_5$) are stable to secondary dissociation. Even a modest partitioning of internal energy to the C_2H_5 fragment leaves the HCCO product below the exit barrier for the quartet dissociation channel.

Nominally, the formation of quartet state HCCO from singlet ethyl ethynyl ether is spin-forbidden. However, spin–orbit coupling between singlet and triplet electronic excited states of ethyl ethynyl ether can result in intersystem crossing to a triplet state of the molecule which can decompose to quartet state HCCO product. We performed preliminary electronic structure calculations[27] to look for evidence of spin–orbit coupling in ethyl ethynyl ether. In order to identify the bright state, transition moments were calculated using CI singles excitations (see Experiment section for details). Although all bright states had vertical excitation energies that were far too high, the two candidate states with large oscillator strengths consistent with the strong absorption band are the $S_4(A'')$ and $S_5(A')$ states. The two dominant electron configurations contributing to the $S_4(A'')$ state result from excitations of electrons from a delocalized CCO out-of-plane π orbital (with CC bonding character and CO anti-bonding character) to two higher orbitals with Rydberg character. The transition to the $S_4(A'')$ state has a slightly higher oscillator strength than the second possibility, the $S_5(A')$ state. The dominant electron configurations of the $S_5(A')$ state result from the excitation of an electron from a delocalized CCO in-plane π orbital (again with CC bonding character and CO anti-bonding character) to the same two higher orbitals with Rydberg character.

Each of these candidate singlet states has an energetically close triplet state in the Franck–Condon region to which it can couple with a significant ($\sim$37 cm^{-1}) spin–orbit coupling matrix element. The $S_4(A'')$ state couples most strongly to the $T_5(A')$ state with $\Delta E(T_5-S_4)=0.2$ eV, whereas the $S_5(A')$ state couples most strongly to the $T_4(A'')$ state with a larger energy difference of $\Delta E(S_5-T_4)=0.9$ eV. The spin–orbit coupling matrix element between the $S_4(A'')$ and $T_5(A')$ states results from a one electron change from an out-of-plane π orbital of a'' symmetry (with CC bonding character and CO anti-bonding character) to a similar π CCO orbital which is in the mirror plane of ethyl ethynyl ether and thus has a' symmetry. The coupling between the $S_5(A')$ and $T_4(A'')$ orbitals also involves a one-electron transition between two sets of delocalized CCO π orbitals with CC bonding character and CO anti-bonding character. In this case, however, the electron moves from the out-of-plane a' orbital to the in-plane a'' orbital. HCCO in the $\tilde{a}(^4A'')$ state could be a product from either of these triplet states. Although the HCCO product has a'' symmetry, this is defined with respect to the HCC plane for bent geometries in the ground state while the plane of symmetry in ethyl ethynyl ether is the COC plane. Thus HCCO with A'' symmetry with respect to the HCC plane could be formed from either $T_4(A'')$ or $T_5(A')$ state of ethyl ethynyl ether. These calculations rationalize production of quartet HCCO from a process which occurs via intersystem crossing to one of the two triplet states discussed above, but higher level electronic structure calculations are needed to thoroughly evaluate the dissociation mechanism.

There are two other C_2HO isomers which might also account for the slow recoil kinetic energy product. One of the C_2HO isomers is the hydroxyethynyl radical, CCOH. Yamaguchi *et al.* have characterized the energy of this radical at several levels of theory.[39] At the highest level used, CCSD(T)—coupled cluster with single and double excitations and perturbative triple excitations, with the largest basis set, TZ3P$(2f,2d)$, the zero-point-corrected energy of the CCOH ground state was calculated at 55.1 kcal/mole above the HCCO ground state. As in the case of the $\tilde{a}$ state, this energy lies close to the 55 kcal/mole edge of the low recoil kinetic-energy distribution and could account for the slow peak in our spectrum. However, it would take a substantial rearrangement for this radical to crack to $m/e=25\,(C_2H^+)$, the dominant daughter ion obtained upon electron bombardment ionization, losing the oxygen but keeping the hydrogen, so this possibility seems unlikely. The other possible C_2HO isomer is a ringed structure known as the oxiryl radical, which was considered as a possible intermediate by Taatjes[40] in a recent study of the CH(CD)$[X\,^2\Pi]+CO$ reaction and also in work of Anderson *et al.*[41] studying the same reaction. The energy of this isomer is not definitively characterized in the literature, so whether it might explain our observed energy distributions is an open question.

Note added in proof. Two groups have done calculations on the oxiryl radical. The energy difference from the zero-point level of ground state HCCO to the zero-point level of the oxiryl radical was found to be 54 kcal/mole (J. L. Durant, private communication of unpublished results, 2000) using density functional methods. This energy difference was found to be 50 kcal/mole (K. W. Sattelmeyer and H. F. Schaefer, private communication of unpublished results, 2003), using equation-of-motion coupled-cluster methods for ionization potentials applied to obtain the neutral ground state from the closed shell anion. Furthermore, Durant has calculated a barrier to isomerization of 3 kcal/mole for the oxiryl radical converting to ground state HCCO. Thus the low recoil kinetic-energy channel cannot be forming the oxiryl radical, because a significant fraction of the radicals would then have sufficient energy to isomerize to the ground state and subsequently dissociate to CH + CO. Since appreciable secondary dissociation to CH + CO was not observed, these energy calculations support the assignment of the low recoil kinetic-energy channel to quartet state ketenyl, as opposed to the oxiryl radical.

ACKNOWLEDGMENTS

This work was supported by the Chemical, Geosciences and Biosciences Division, Office of Basic Energy Sciences, Office of Science, U.S. Department of Energy, under Grant Nos. DE-FG02-92ER14305 (L.J.B.) and DE-FG02-86ER13492 (R.B). M. J. K. acknowledges a National Science Foundation Graduate Research Fellowship. The Advanced Light Source is supported by the Director, Office of Science, Office of Basic Energy Sciences, Materials Sciences Division, of the U.S. Department of Energy under Contract No. DE-AC03-76SF00098 at Lawrence Berkeley National Laboratory. The Chemical Dynamics Beamline is supported by the Director, Office of Science, Office of Basic Energy Sciences, Chemical Sciences Division of the U.S. Department of Energy under the same contract. The authors would like to thank Laura R. McCunn for her extensive background research on ethyl ethynyl ether, Bradley F. Parsons for his guidance with the spin–orbit coupling matrix calculations and David E. Szpunar for his help with the initial data acquisition at Chicago. We are also indebted to Branko M. Ruscic for his calculations exploring the $\tilde{A}$ state of the ketenyl radical.

[1] C. P. Fenimore and G. W. Jones, J. Chem. Phys. **39**, 1514 (1963).
[2] J. V. Michael and A. F. Wagner, J. Phys. Chem. **94**, 2453 (1990), and references therein.
[3] A. M. Schmoltner, P. M. Chu, and Y. T. Lee, J. Chem. Phys. **91**, 5365 (1989).
[4] J. A. Miller, R. J. Kee, and C. K. Westbrook, Annu. Rev. Phys. Chem. **41**, 345 (1990), and references therein.
[5] K. T. Rim and J. F. Hershberger, J. Phys. Chem. A **104**, 293 (2000).
[6] K. G. Unfried, G. P. Glass, and R. F. Curl, Chem. Phys. Lett. **177**, 33 (1991).
[7] G. P. Glass, S. S. Kumaran, and J. V. Michael, J. Phys. Chem. A **104**, 8360 (2000).
[8] J. Grußdorf, J. Nolte, F. Temps, and H. G. Wagner, Ber. Bunsenges. Phys. Chem. **98**, 546 (1994).
[9] M. A. Edwards and J. F. Hershberger, Chem. Phys. **234**, 231 (1998).
[10] M. L. Morton, D. E. Szpunar, and L. J. Butler, J. Chem. Phys. **115**, 204 (2001).
[11] R. Bersohn, J. Chin. Chem. Soc. (Taipei) **49**, 291 (2002). Please note that the HCCO precursor listed in Table III, methyl ethynyl ether, is not commercially available, while ethyl ethynyl ether is.
[12] M. J. Molera, J. M. Gamboa, J. A. García Domínguez, and A. Couto, J. Gas Chromatography **6**, 594 (1968).
[13] T. J. Lee, D. J. Fox, H. F. Schaefer III, and R. M. Pitzer, J. Chem. Phys. **81**, 356 (1984).
[14] J. D. Goddard, Chem. Phys. Lett. **154**, 387 (1989).
[15] P. G. Szalay, J. F. Stanton, and R. J. Bartlett, Chem. Phys. Lett. **193**, 573 (1992).
[16] P. G. Szalay, G. Forgarasi, and L. Nemes, Chem. Phys. Lett. **263**, 91 (1996).
[17] Y. Endo and E. Hirota, J. Chem. Phys. **86**, 4319 (1987).
[18] P. G. Szalay and J.-P. Blaudeau, J. Chem. Phys. **106**, 436 (1997).
[19] N. R. Forde, T. L. Myers, and L. J. Butler, Faraday Discuss. **108**, 221 (1997).
[20] L. R. Brock, B. Mischler, and E. A. Rohlfing, J. Chem. Phys. **110**, 6773 (1999).
[21] L. R. Brock, B. Mischler, and E. A. Rohlfing, J. Chem. Phys. **107**, 665 (1997).
[22] C. Hu, H. F. Schaefer III, Z. Hou, and K. D. Bayes, J. Am. Chem. Soc. **115**, 6904 (1993).
[23] P. A. Heimann, M. Koike, C. W. Hsu, D. Blank, X. M. Yang, A. G. Suits, Y. T. Lee, M. Evans, C. Y. Ng, C. Flaim, and H. A. Padmore, Rev. Sci. Instrum. **68**, 1945 (1997); X. Yang, J. Lin, Y. T. Lee, D. A. Blank, A. G. Suits, and A. M. Wodtke, *ibid.* **68**, 3317 (1997).
[24] D. Peterka and M. Ahmed (personal communication).
[25] M. J. Frisch, G. W. Trucks, H. B. Schlegel *et al.*, GAUSSIAN 98, Revision A.11.3., Gaussian, Inc., Pittsburgh, PA, 2002.
[26] A. G. Baboul, L. A. Curtiss, P. C. Redfern, and K. Raghavachari, J. Chem. Phys. **110**, 7650 (1999).
[27] M. W. Schmidt, K. K. Baldridge, J. A. Boatz *et al.*, J. Comput. Chem. **14**, 1347 (1993).
[28] H. M. Rosenstock, K. Draxl, B. W. Steiner, and J. T. Herron, in *NIST Chemistry WebBook, NIST Standard Reference Database Number 69*, edited by P. J. Linstrom and W. G. Mallard (National Institute of Standards and Technology, Gaithersburg, MD 20899 (http://webbook.nist.gov), July, 2001).
[29] S. G. Lias, in *NIST Chemistry WebBook, NIST Standard Reference Database Number 69*, edited by P. J. Linstrom and W. G. Mallard (National Institute of Standards and Technology, Gaithersburg, MD, 20899 (http://webbook.nist.gov), July, 2001.
[30] S. S. E. NIST Mass Spec Data Center, director, in *NIST Chemistry WebBook, NIST Standard Reference Database Number 69*, edited by P. J.

Linstrom and W. G. Mallard (National Institute of Standards and Technology, Gaithersburg, MD 20899 (http://webbook.nist.gov), July 2001.
[31] W. Tsang, in *Energetics of organic free radicals*, edited by J. A. M. Simões, A. Greenberg, and J. F. Liebman (Blackie Academic & Professional, London, 1996), pp. 22.
[32] D. L. Osborn, D. H. Mordaunt, H. Choi, R. T. Bise, and D. M. Neumark, J. Chem. Phys. **106**, 10087 (1997).
[33] D. H. Mordaunt, D. L. Osborn, H. Choi, R. T. Bise, and D. M. Neumark, J. Chem. Phys. **105**, 6078 (1996).
[34] R. Sustmann, W. Sicking, and M. Felderhoff, Tetrahedron **46**, 783 (1990).
[35] J. B. Foresman and A. Frisch, *Exploring chemistry with electronic structure methods*, 2nd ed. (Gaussian, Inc., Pittsburg, PA, 1996).
[36] D. L. Osborn, J. Phys. Chem. A **107**, 3728 (2003).
[37] A. Kasdan, E. Heerbst, and W. C. Lineberger, Chem. Phys. Lett. **31**, 78 (1975).
[38] D. R. Yarkony, J. Phys. Chem. **100**, 17439 (1996).
[39] Y. Yamaguchi, J. C. Rienstra-Kiracofe, J. C. Stephens, and H. F. Schaefer III, Chem. Phys. Lett. **291**, 509 (1998).
[40] C. A. Taatjes, J. Chem. Phys. **106**, 1786 (1997).
[41] S. M. Anderson, K. E. McCurdy, and C. E. Kolb, J. Phys. Chem. **93**, 1042 (1989).